Nonlinear *B–H* Curves

TABLE B.1   Constants for $\mu = B/H = [1/(k_1\, e^{k_2\, B^2} + k_3)] + \mu_o$ furnished by Mark A. Juds with permission of Eaton Corporation. Note that these are all approximate and highly dependent on manufacturing methods, etc.

Ferromagnetic Material	k_1	k_2	k_3
1010 annealed—US Steel	4.847	1.908	227.3
1010 cold rolled—US Steel	36.62	1.331	534.9
1020 annealed—US Steel	4.770	2.055	302.2
1020 cold rolled—US Steel	14.23	1.699	806.5
1030 annealed—US Steel	50.00	1.371	645.3
1030 cold rolled—US Steel	40.00	1.416	1212.
Armco® H0	0.00001500	4.650	11.08
Armco M6	0.006819	3.195	10.59
Armco M15	0.8795	2.666	94.27
Armco M19	2.150	2.477	83.03
Armco M22	2.214	2.412	90.38
Armco M36	1.683	2.432	103.5
Armco M45	3.500	2.148	124.8
Armco M47	0.1247	3.335	70.83
Carpenter® Hiperco® 15	5.137	1.700	389.8
Carpenter Hiperco 50 A	0.0009388	2.816	49.92
Carpenter HiPerm® 49 annealed	0.001857	6.265	8.250
Carpenter HiPerm 49 mill processed	53.86	0.9941	149.3
Carpenter HiMu® 80	0.0002031	26.73	1.858
Carpenter HiMu 800	0.00002000	31.32	2.758
Carpenter silicon core iron B-FM	1.192	2.812	174.5
Cast iron gray—Metals HDBK	4093	0.9865	142.1
Cast iron nodular—Metals HDBK	55.04	2.324	1630
Magnetics® SqPermalloy	0.04500	9.091	6.344

(*continued*)

TABLE B.1 (*Continued*)

| Ferromagnetic Material	k_1	k_2	k_3
Magnetics Supermalloy®	0.1073	9.176	3.046
Magnetics Supermendur®	0.03715	0.9109	11.12
Metglas® 2605S-2	0.00003232	5.632	2.164
Metglas 2605S-3A	0.0007339	5.178	1.588
Metglas 2605SM	0.003031	6.138	1.171
Metglas 2826MB	0.00002981	17.82	0.9301
Micrometals 26	2000	1.092	889.4
Micrometals 52	2002	1.023	1901
Stainless steel 416—Metals HDBK	11.92	2.749	1036
Stainless steel 430F $H_{RB} = 78$—Carpenter	0.01186	7.701	418.2
Stainless steel 430F $H_{RB} = 87$—Carpenter	0.1384	6.117	708.9
Stainless steel 430FR 9.53 mm Dia–Carpenter	0.02981	6.880	407.4
Stainless steel 430FR 15.9 mm Dia–Carpenter	0.01375	8.428	723.5
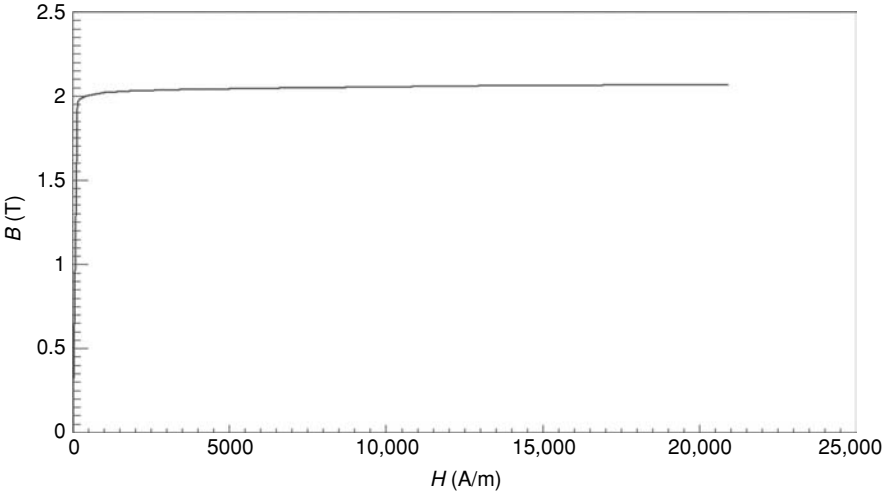
FIGURE B.1   "Step" *B–H* curve suitable for finite-element analysis, in which the slope below 1.93 T is 10,000 times the permeability of free space and the slope above 2 T approaches the permeability of free space. The data points are in Table B.2.1.

TABLE B.2.1   Data points for "step" *B–H* curve of Figure B.1.

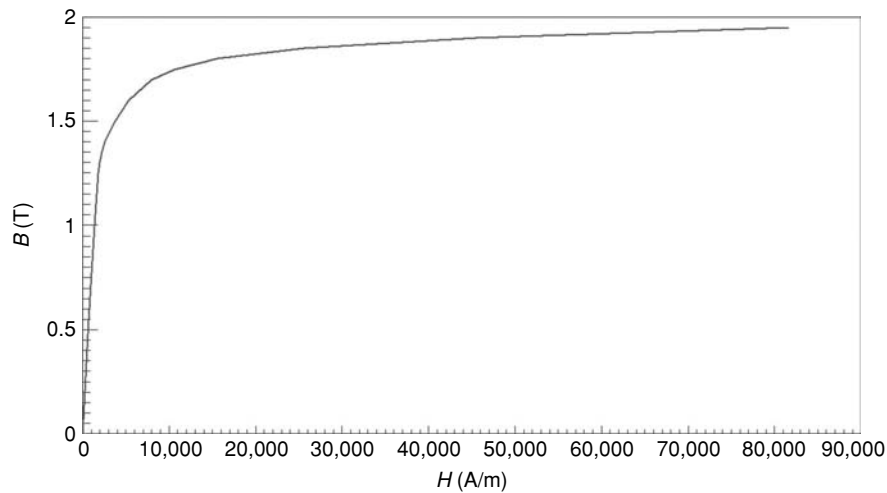| B (teslas)	H (A/m)
0	0
1.93	153.5
1.94	155.1
1.95	158.3
1.96	164.7
1.97	177.4
1.98	202.9
1.99	304.9
2.00	406.9
2.01	610.9
2.02	1009
2.03	1805
2.04	3396
2.05	6578
2.06	12,942
2.07	20,897

FIGURE B.2   Real *B–H* curve used for finite-element analysis of cylindrical plunger and stopper of the Bessho actuator. The relative permeability for $B < 0.55$ T is $(0.55/695)/12.57\text{E}{-}7 = 630$. The data points are in Table B.2.2.

TABLE B.2.2   Data points for "real" *B–H* curve of Figure B.2.

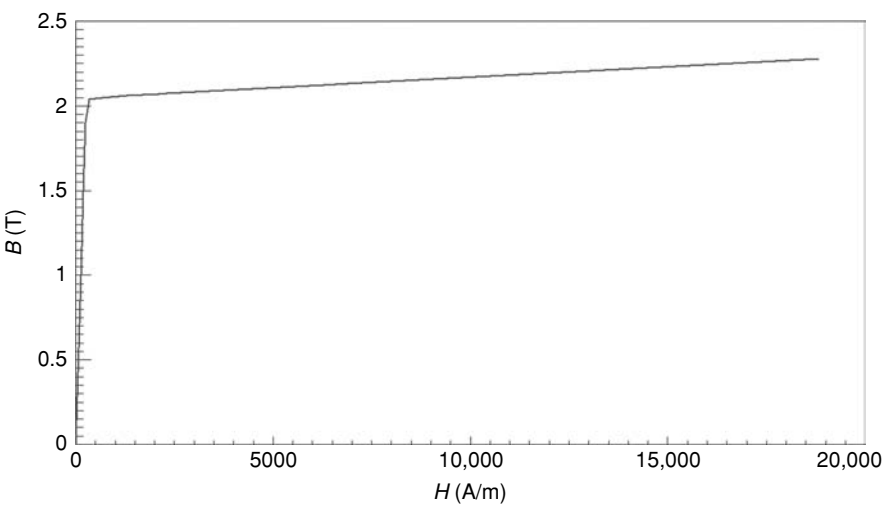| B (teslas)	H (A/m)
0	0
0.55	695
1.0	1350
1.15	1600
1.25	1800
1.3	1950
1.35	2200
1.4	2600
1.5	3800
1.6	5300
1.7	8000
1.75	10,652
1.8	15,624
1.85	25,568
1.9	45,457
1.95	81,618
1.96026	89,780
2.15513	244,854

FIGURE B.3   Ramp *B–H* curve used for finite-element analysis. The relative permeability of the initial ramp is 630, and of the final ramp is 1. See Table B.2.3 for data points.

TABLE B.2.3   Data points for ramp *B–H* curve of Figure B.3.

B (teslas)	*H* (A/m)
0	0
1.0	1263
1.5	1894
1.9	2399
2.04	3396
2.05	6578
2.06	12,942
2.07	20,897
2.07263	22,987
2.12253	62,691
2.13041	68,960
2.28009	188,073